



PII S0016-7037(97)00085-9

The nature and origin of rims on lunar soil grains

LINDSAY P. KELLER¹ and DAVID S. MCKAY²¹MVA, Inc., 5500 Oakbrook Parkway, Suite 200, Norcross, Georgia 30093, USA²Code SN, Solar System Exploration Division, NASA Johnson Space Center, Houston, Texas 77058, USA*(Received May 9, 1996; accepted in revised form February 11, 1997)*

Abstract—Space weathering processes that operate in the lunar regolith modify the surfaces of lunar soil grains. Transmission electron microscope analysis of the lunar soil grains from the fine size fraction of several lunar soils show that most grains are surrounded by thin (60–200 nm thick) rims. The microstructure and chemical compositions of the rims can be used to classify rims into four broad categories: amorphous, inclusion-rich, multiple, and vesicular. Amorphous rims are noncrystalline, generally lack crystalline inclusions, show evidence for preferential sputtering of cations, and are produced largely by solar-wind irradiation damage. Inclusion-rich rims contain abundant nanometer-sized grains of Fe metal as randomly dispersed inclusions or as distinct layers embedded in an amorphous silica-rich matrix. Inclusion-rich rims are compositionally distinct from their host grains and typically contain accumulations of elements that are not indigenous to the host. Inclusion-rich rims are formed largely by the deposition of impact-generated vapors with a contribution from the deposition of sputtered ions. A continuum in the chemical and microstructural properties exists between typical amorphous rims and typical inclusion-rich rims. Multiple-rims consist of a distinct radiation-damaged layer up to 50 nm thick, that is overlain by vapor-deposited material of comparable thickness. Vesicular rims are compositionally similar to their hosts and are characterized by an abundance of small (<50 nm in diameter) vesicles concentrated in the outer 100 nm of the rims. The formation of vesicular rims is apparently due to the evolution of solar-wind implanted gases in response to a pulse-heating event.

The formation of rims on lunar soils is complex and involves several processes whose effects may be superimposed. From this study, it is shown that one process does not dominate and that the relative importance of vapor-deposition is comparable to radiation-damage in the formation of rims on lunar silicate grains. The presence of rims on lunar soil grains, particularly those with nanometer-sized Fe metal inclusions, may have a major influence on the optical and magnetic properties of lunar soils.
Copyright © 1997 Elsevier Science Ltd

1. INTRODUCTION

Rocks and soils in the lunar regolith exposed at the Moon's surface are subjected to a variety of processes which result in modifications to their surfaces. Micrometeorite impacts can result in shock, melting, vaporization, the burial of the target, and the excavation of buried materials (McKay et al., 1991). The presence of abundant agglutinates and impact glasses in the lunar soil is testimony to the magnitude of this effect. In addition to the impact-processing, lunar materials exposed directly to the Sun become implanted with high concentrations of low-mass solar-wind ions (H, He, C, etc.) to a depth of a few tens of nanometers from their surfaces. Exposure to the Sun also results in damage from heavy ions from solar flares, which, along with cosmic rays, leave latent tracks in grains (Walker, 1980). An understanding of the dynamics of grain surfaces in the regolith are important for understanding space weathering effects (e.g., Pieters et al., 1993), inferring past solar activity, and characterizing regolith evolution on airless bodies.

A distinctive microscopic feature of lunar soil grains was discovered soon after the return of the first Apollo samples, when high-voltage transmission electron microscope (HVTEM) observations showed that many soil grains were surrounded by thin amorphous rims (e.g., Dran et al., 1970; Bibring et al., 1972). These results, when combined with laboratory experiments on artificially irradiated grains, demonstrated that amorphous rims could form in response to the

implantation of ions with solar wind energies. However, at the time that the HVTEM measurements were made, the technology to determine the chemical composition of amorphous rims directly in the transmission electron microscope (TEM) did not exist. Other types of analysis, however, showed that the surfaces of soil grains were enriched in certain elements above the bulk soil values. The results from surface analysis techniques led to the hypothesis that a deposited component (either sputter-deposition or the condensation of impact-derived vapors) was present on the surfaces of lunar soil grains. Thus, it was not clear from the surface analysis studies (Gold et al., 1975; Housley and Grant, 1976, 1977; Dikov et al., 1978) or ion microprobe measurements (Zinner et al., 1978), whether irradiation or vapor deposition was the major mechanism of grain surface modification. The isotopic data obtained from lunar soils was also somewhat equivocal. Early results suggested that the grain surfaces of lunar soils were enriched in the heavy isotopes of O, Si, S, and K (e.g., Epstein and Taylor, 1972; Clayton et al., 1974; Kerridge and Kaplan, 1978), and various models were considered to explain the apparent loss of the light isotopes of these elements from the Moon. However, more recent isotopic measurements for Ca and Mg (two elements with markedly different volatilities) show insignificant fractionation effects (Russell et al., 1977; Esat and Taylor, 1992). It has been suggested that the large effects for Si and O are artifacts of the analysis (Esat and Taylor, 1992); however, the S isotope data are unequivocal and implicate a surface-depos-

ited component. The debate among the various hypotheses was quite contentious, but by the early 1980s, the general consensus was that rims were formed largely by irradiation.

Recent work challenged the radiation model for the formation of amorphous rims because of developments in sample preparation techniques, along with new generations of X-ray detectors for TEMs (Keller and McKay, 1993). For the first time, the compositions of amorphous rims were measured along with observations of their microstructure. The results of Keller and McKay (1993) demonstrated that the compositions of rims differed significantly from the compositions of the host grains, and led to the hypothesis that much of the "thickness" of the amorphous rims was material that condensed from impact-generated vapors. These results, however, were soon challenged by Bernatowicz et al. (1994a) who maintained that rims were still largely formed by irradiation, based on observations of soil ilmenites. Bernatowicz et al. (1994a) suggested that vapor deposition is a democratic process (e.g., all soil grains behave similarly) and that the relative importance of vapor deposition compared to radiation damage could be evaluated by analyzing the rims on ilmenite. They showed that while silicate-rich vapor deposits were present on the ilmenite surfaces, the volume of deposited material was small relative to the radiation damaged material. Keller and McKay (1994a,b) and Christoffersen et al. (1994) countered that ilmenite grains behave differently than the silicates in lunar soils. Thus, in the ensuing debate (Bernatowicz et al., 1994b; Keller and McKay, 1994a,b) the exact nature of amorphous rims was not resolved.

The controversy over rim formation mechanisms can potentially be clarified by applying a recent discovery in the analysis of interplanetary dust particles (IDPs). Bradley (1994a) analyzed "sputtered rims" on IDPs and detected a particular chemical signature of the sputtering process on silicates. These analyses suggested that prolonged irradiation of ferromagnesian silicates resulted in a marked depletion in some cations (especially Mg) relative to the other elements in the host grain. The observed cation depletion was manifested as a stoichiometric excess of oxygen in the analysis. Subsequent experiments on the proton and helium irradiation of Fe-bearing olivine showed similar chemical effects, and indicated that, for certain silicates, the response to irradiation is the preferential sputtering of cations with the lowest binding energy (Bradley, 1994a; Bradley et al., 1996). These results have important implications for the amorphous rims on lunar soil grains because lunar grains have been exposed to approximately the same radiation environment for similar periods of time as compared to IDPs. In light of this background, we have expanded on our earlier work by obtaining detailed analyses of the composition (including quantitative O abundances) and microstructures of rims on lunar soil silicate grains.

2. METHODS

Aliquots consisting of a few hundred grains from the fine-size fractions (typically $<20 \mu\text{m}$ or $<10 \mu\text{m}$ fractions) of several lunar soils were analyzed (including 10084, 72881, 72501, 61181, and 61221). These aliquots were embedded in low viscosity epoxy (Embed 812) and TEM specimens were prepared using an ultramicrotome to cut thin sections $\sim 50\text{--}80 \text{ nm}$ thick. These sections were



Fig. 1. A dark-field TEM image of an amorphous rim on a plagioclase grain from soil 72501. The linear features in the core of the grain are solar flare tracks. The irregular interface between the rim and host is a likely irradiation effect (see text).

placed on copper TEM grids that were covered with continuous, amorphous-carbon thin films. The thin sections were analyzed in a JEOL 2010 (200 keV) transmission electron microscope (TEM) equipped with a Noran thin-window energy-dispersive X-ray (EDX) spectrometer and a GATAN parallel electron energy-loss spectrometer (PEELS). Quantitative EDX analyses were obtained using the Cliff-Lorimer thin-film analysis method with experimental k-factors obtained from a variety of synthetic and mineral standards including NIST-SRM-2063 thin film standard, troilite, and Ni_2SiO_4 (details given in Bradley, 1994b). The EDX spectra were collected such that the errors based upon counting statistics were $<3\%$ for major elements. Feldspars were analyzed with low beam currents in order to avoid beam damage which can cause element diffusion away from the analysis volume. Special precautions were taken in the quantitative analysis for oxygen because of the well-known problems with preferential absorption of oxygen X-rays in samples which are too thick. For the analyses reported here, we only accepted analyses of rims where the analysis of the corresponding substrate demonstrated oxygen stoichiometry (i.e., there were no absorption effects for oxygen in the host grain). In this way, we used the substrate stoichiometry as an internal "check" for absorption problems in the quantitative analysis of oxygen.

3. RESULTS

The common constituents of the fine size fraction of lunar soils includes mineral grains, glass, lithic fragments, agglutinate fragments, and spherules. Preliminary examination of the ultramicrotome thin sections showed that many, but not all, of the soil grains are surrounded by thin (50–200 nm thick) rims that are distinct from their hosts. More detailed transmission electron microscope analysis revealed that the rims on lunar soil grains are not uniform and homogeneous from grain to grain but are, in fact, a diverse collection with widely varying microstructures and chemical compositions. While acknowledging that there exists considerable variability and range of properties within and among the groups, we use these characteristics to delineate four broad groups of rims based upon their microstructure and chemistry: amorphous, inclusion-rich, multiple, and vesicular. Most rims on lunar soil grains fall into the first two categories.

3.1. Amorphous Rims

Figure 1 illustrates a typical amorphous rim on a plagioclase grain from soil 72501. The mottled contrast in the core

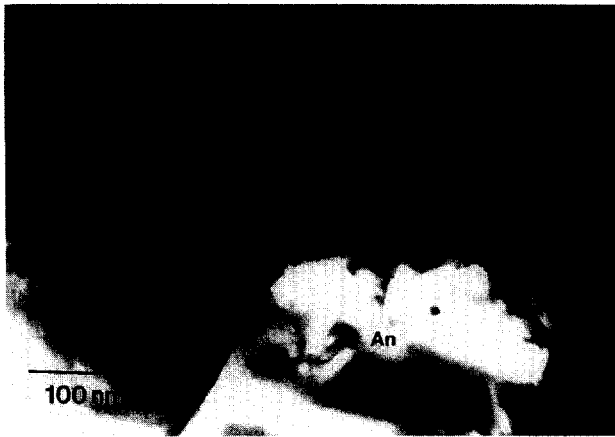


Fig. 2. A dark-field TEM image of an amorphous rim on plagioclase showing the amorphous and featureless nature of the rim microstructure.

of the host plagioclase grain results from the high density of solar flare tracks that are present within the grain ($\sim 1 \times 10^{11} \text{ cm}^{-2}$), while the fractures are a microtomy artifact. Dark-field TEM imaging confirms that the rims are truly amorphous and lack any long-range crystalline order (Fig. 2). Amorphous rims on lunar soil grains show a range of apparent rim thicknesses from ~ 20 to 100 nm, but on average are ~ 60 nm thick. Sparse, fine-grained ($< 1-5$ nm diameter) Fe metal grains are dispersed as inclusions in these rims and are occasionally concentrated as thin surface layers. The interface between the amorphous rims and their crystalline hosts are abrupt on the nanometer-scale and range from very smooth to others with considerable topography, especially for those host grains with a high density of solar flare tracks (Figs. 1 and 2). The formation of these irregular interfaces is enigmatic, but an association with radiation effects has been suggested (Bradley et al., 1996). Amorphous rims have been observed surrounding plagioclase, cristobalite, and orthopyroxene. The chemical systematics of the rim compositions are described below. We were unable to determine whether compositional gradients exist in the amorphous rims largely because of problems with electron irradiation damage with a highly focussed electron probe in the TEM. Use of a small incident probe ($\sim 10-20$ nm diameter) resulted in significant beam-damage with beam currents suitable for microanalysis. (In this respect, the lunar rims differ from IDP rims in their relative beam sensitivity.)

The major element compositions of amorphous rims and their crystalline hosts are generally similar, although the proportions of the elements are typically quite different (for

example, amorphous rims on plagioclase contain major Ca, Al, Si, and O, but in abundances that differ from the host). All amorphous rims analyzed to date contain at least some chemical constituents that are not indigenous to the substrate (i.e., the host grain), the most common of which is Fe. These "foreign" elements are a minor, yet ubiquitous component of amorphous rims (Table 1). The compositions of the amorphous rim and plagioclase host shown in Fig. 2 are presented in Table 1. Relative to the host plagioclase, the rim is depleted in Al by $\sim 50\%$ and Ca by $\sim 80\%$, while the Si/O ratio remains relatively constant (analyses 210–211, Table 1). The loss of cations in the rim manifests itself as superstoichiometry of oxygen relative to the remaining cations; i.e., there are insufficient cations to balance the analytical oxygen. The amount of "excess" O in the previous example is ~ 12 at% and is presumed to be bound to hydrogen in the form of hydroxyl (e.g., Zeller et al., 1966; Bibring et al., 1982; Bradley, 1994a).

The amorphous rims observed on orthopyroxene grains from lunar soils show similar cation depletion and oxygen super-stoichiometry effects as described previously for opx in IDPs. A typical example of a rim-host pair is given in Table 1. The main compositional difference between the amorphous rim and the host orthopyroxene is the dramatic depletion of Mg in the former (by $\sim 80\%$), relative to the host. The magnitude of the oxygen "excess" is ~ 15 at% and is comparable to that observed in rims on plagioclase. The Si/O ratio is the same (within analytical uncertainty) for amorphous rims on opx and their hosts.

True amorphous rims also occur on cristobalite grains, but show a somewhat different behavior as compared to plagioclase and pyroxenes. In cristobalite, the amorphous rims show no statistical difference in their Si/O ratios relative to the host grains; i.e., there is no oxygen superstoichiometry (analyses 6184–6185, Table 1) and the rim compositions are nearly identical to the host grains. Like certain of the plagioclase grains, some of the track-rich cristobalites display the irregular microstructure at the rim-host interface.

3.2. Inclusion-Rich Rims

Inclusion-rich rims are another major variety of rims observed on lunar soil grains; these rims are characterized by an abundance of submicrometer crystalline inclusions of Fe-metal (kamacite), ilmenite (FeTiO_3), and rare Fe-sulfides dispersed in an amorphous, silicate matrix (Figs. 3–6). These inclusion-rich rims are distinguished from accretionary materials such as "pancakes," splash glass, etc., by their lateral extent (they typically completely surround soil grains). Although these rims show a range of apparent thick-

Table 1. Quantitative TEM-EDX analyses of selected amorphous rims and their substrates in lunar soils.

Analysis	(at%)	O	Mg	Al	Si	S	Ca	Ti	Fe
34	rim	67.7	3.43	2.49	21.9	0.38	0.81	0.53	2.80
36	core (opx)	60.2	14.9	0.31	19.8	0.01	0.84	0.07	3.94
211	rim	68.6	0.58	7.16	21.8	0.00	1.52	0.00	0.29
210	core (An)	60.8	0.40	15.7	15.8	0.00	7.30	0.00	0.01
6185	rim	64.3	0.20	0.32	35.2	0.00	0.01	0.00	0.01
6184	core (crst)	63.8	0.18	0.37	35.6	0.00	0.06	0.00	0.00

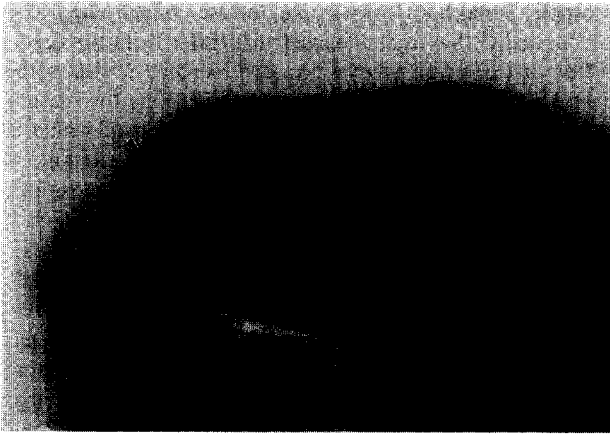


Fig. 3. A bright-field TEM image of an inclusion-rich rim on plagioclase from soil 10084. The dark inclusions in the rim are nanometer-sized Fe metal, some of which are concentrated into thin layers within the rim.

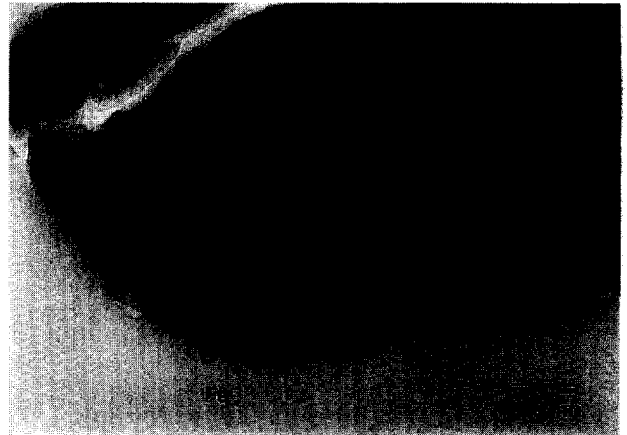


Fig. 5. A bright-field TEM image of a thick (~ 200 nm), inclusion-rich rim on plagioclase showing both coarse- and fine-grained Fe metal inclusions in discrete layers within the rim.

nesses (from ~ 40 to over 200 nm), they comprise the majority of rims with thicknesses exceeding 100 nm. The inclusions are either randomly dispersed throughout the thickness of the rim (Fig. 4), or occur as discrete layers of inclusions, either single (Fig. 6) or multiple layers (Figs. 3 and 5) within the rim thickness or at the rim surface. The size distribution of inclusions also shows considerable variability. The majority of Fe inclusions are single crystals, circular in cross-section, and typically < 10 nm in diameter (e.g., Fig. 3), placing them at the lower end of the size range of much of the single-domain Fe also found in agglutinitic glass (Housley et al., 1973; Fallick et al., 1983; Keller and McKay, 1994c). Spherical inclusions of kamacite up to 50 nm in diameter occur in some rims (Figs. 4 and 5). The interfaces between most inclusion-rich rims and their substrates are typically smooth and lack the irregular microstructure described above for typical amorphous rims.

The compositions of the inclusion-rich rims are complex and tend to be quite dissimilar to the host grain (see Table 2). Inclusion-rich rims have been observed on plagioclase,

opx, cpx, cristobalite, and ilmenite and, regardless of the substrate mineralogy, all examples of inclusion-rich rims show significant accumulations of elements that are not indigenous to the host grain. Furthermore, none of the analyzed rims of this type show the oxygen superstoichiometry that occurs in most of the amorphous rims described above. For example, the inclusion-rich rim and its host shown in Fig. 3 display the following chemical characteristics: (1) the rim contains Mg, S, Ti, and Fe which were either not detected in the host plagioclase or occurred in trace quantities, (2) while Al is depleted in the rim relative to the host, Si is enriched, and Ca appears unchanged, and (3) oxygen is depleted in the rim relative to the host by $\sim 20\%$ (Table 2). The reported oxygen concentration for the rims given in Table 2 reflect the assumption that all the Fe in the rim is either in metallic form, or bonded with S. The Si/O ratio is much higher in the rim than in the host. In this case, where a large oxygen deficiency is observed (analysis 242, Table 2), a reduced silicon valency is required in order to achieve stoichiometry. We used electron energy-loss spectroscopy (EELS) to study the Si-bonding environment in inclusion-

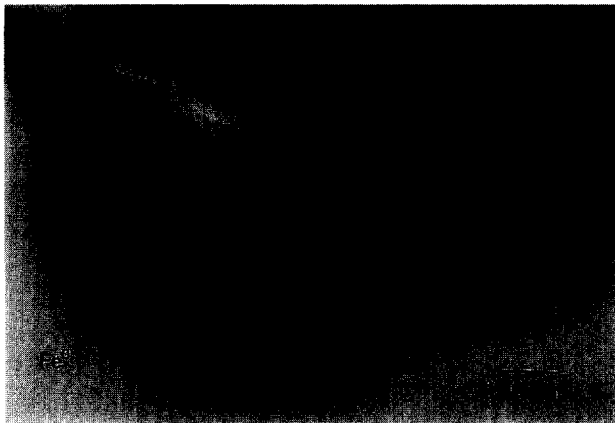


Fig. 4. A bright-field TEM image of a thick (~ 150 nm), inclusion-rich rim on plagioclase from soil 61181 that contains large (~ 50 nm in diameter) inclusions of Fe metal (indicated with arrows).



Fig. 6. A bright-field TEM image of an inclusion-rich rim with a concentration of Fe metal grains at the uppermost surface.

Table 2. Quantitative TEM-EDX analyses of selected inclusion-rich rims and their substrates in lunar soils.

Analysis	(at%)	O	Mg	Al	Si	S	Ca	Ti	Fe
242	rim	52.7	5.36	12.4	18.5	0.04	7.03	0.50	3.54
243	core (An)	61.0	0.51	15.6	16.2	0.00	6.74	0.00	0.00
21	rim	60.9	3.59	4.13	25.9	0.27	1.68	0.72	2.82
20	core (opx)	60.2	13.3	0.53	20.5	0.00	1.50	0.16	3.91
165	rim	57.0	5.75	7.58	18.2	0.21	4.63	1.38	5.29
164	core (cpx)	59.0	8.11	0.84	19.0	0.00	5.26	0.22	7.57
171	outer rim	57.8	6.75	9.24	16.3	0.31	4.55	0.73	4.35
170	core (crst)	65.3	0.04	0.40	34.2	0.00	0.00	0.00	0.00

rich rims, but were unable to independently verify the presence of multiple valence states for Si.

The compositions of inclusion-rich rims on cristobalite are distinct from the host and are in stark contrast to the amorphous rims on cristobalite that were described above. Relative to the host grain, the inclusion-rich rim on cristobalite contains abundant Mg, Al, S, Ca, Ti, and Fe, and has a much lower Si/O ratio (Table 2). The inclusion-rich rim compositions on both plagioclase and cristobalite from the same soil are very similar (Table 2).

Like the rims on cristobalite, rims on ilmenite grains contain high concentrations of elements that are not present above trace levels in the host. However, unlike silicate grains, the interface between the rim and substrate is diffuse and difficult to see in images (Christoffersen et al., 1994, 1996).

3.3. Multiple Rims

One of the intriguing results of this work was the identification of multiple rims on soil grains consisting of discrete layers that are microstructurally and chemically distinct from one another. Figure 7a and b shows a multiple rim on a track-rich plagioclase grain. The inner rim is ~40 nm thick and has the chemical and microstructural characteristics of the amorphous rims described above (see analyses 153–155, Table 3). The inner rim shares an irregular interface with the host grain, is amorphous, and lacks crystalline inclusions. The composition of the inner rim is similar to the host grain except for substantial depletions in Al and Ca, and a slight oxygen superstoichiometry. An outer rim (~40–50 nm thick) lies on top of the inner rim. The outer rim contains abundant crystalline inclusions of Fe metal and ilmenite and has a distinctly different composition relative to the host grain and the inner rim (Table 3). The interface between the inner and outer rim is smooth and abrupt. Although these multiple rims are not common in the analyzed soils, they preserve important information on the processes involved in their formation. Multiple rims have been observed on plagioclase, orthopyroxene, and cristobalite.

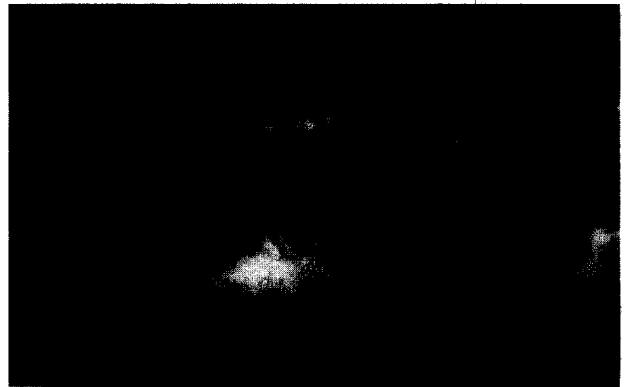
An unusual form of multiple rim is observed on soil ilmenite grains. Several workers have documented that ilmenites have a radiation-processed rim (up to 100 nm thick) and an outer, thinner veneer of silica-rich material that is inferred to be vapor-deposited material (Bernatowicz et al., 1994a; Christoffersen et al., 1994). The inner, radiation-damaged rim is microcrystalline, depleted in Fe and O, and contains Fe and Ti in reduced forms. Superimposed on the radiation-

damaged rim is a layer of amorphous silicate material with inclusions of fine-grained Fe metal.

3.4. Vesicular Rims

Many of the soil grains (both glass and mineral fragments) in fine size fractions of lunar soils (especially 61221 and 10084) are surrounded by what we term “vesicular rims” that are typically ~100 nm wide (Fig. 8). These rims are amorphous and do not contain visible inclusions (e.g., Fe metal grains). Their main structural characteristic is an abun-

(a)



(b)

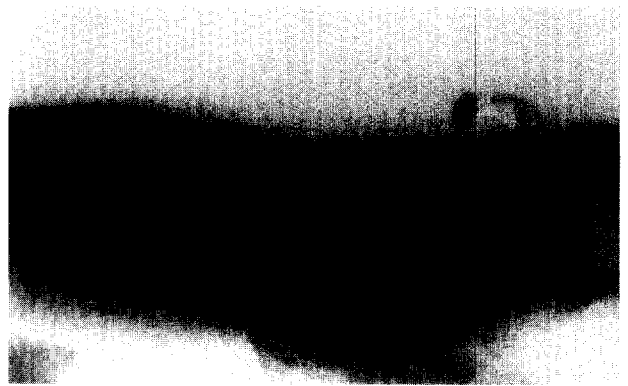


Fig. 7. (a) A dark-field TEM image of a multiple rim on plagioclase from soil 78221. The linear features in the core of the grain are solar flare tracks. The extent of the inner, radiation produced rim, and the outer, vapor-deposited rim are indicated. (b) The corresponding bright-field TEM image of (a). The dark inclusions in the outer rim are a mixture of Fe metal and ilmenite grains. Note the abrupt interface between the inner and outer rims.

Table 3. Quantitative TEM-EDX analyses of selected multiple rims and their substrates in lunar soils.

Analysis	(at%)	O	Mg	Al	Si	S	Ca	Ti	Fe
155	outer rim	58.3	5.96	5.31	14.7	0.20	4.54	4.36	6.67
154	inner rim	62.2	0.76	11.9	20.6	0.04	3.69	0.34	0.50
153	core (An)	60.7	0.18	15.8	16.0	0.00	7.28	0.00	0.04
171	outer rim	57.8	6.75	9.24	16.3	0.31	4.55	0.73	4.35
172	inner rim	63.6	0.39	0.64	34.8	0.04	0.23	0.05	0.24
170	core (crst)	65.3	0.04	0.40	34.2	0.00	0.00	0.00	0.00
57	outer rim	56.2	1.50	1.70	14.3	0.33	0.90	17.3	7.80
58	inner rim	61.8	1.60	0.30	2.0	0.21	0.10	30.3	3.50
60	core (ilm)	62.9	0.80	0.00	0.4	0.00	0.00	18.9	17.0

dance of small diameter (<50 nm) vesicles that are concentrated within a 100 nm rim surrounding the grains. Although our current number of analyses are limited, some chemical systematics are apparent. On average, the rim compositions are little different from the core of the grains. However, the data from two pyroxene grains that are surrounded by vesicular rims (Table 4), show that the rims are depleted in certain cations (notably Mg, Ca, and Fe) relative to the core and show slight oxygen superstoichiometry.

4. DISCUSSION AND IMPLICATIONS

The wide range in the chemical and microstructural properties of rims surrounding lunar soil grains is a strong argument for multiple formation processes. From past research, it is known that a number of processes are operating in the lunar regolith that lead to modifications to grain surfaces. In fact, much of the past debate has been over the relative contributions of these processes. The fact that soil grains are exposed to the Sun leads to implantation effects and strong interactions between the mineral grains and ionizing radiation. Maurette and coworkers demonstrated that exposing mineral grains to a high flux of low energy ions (equivalent to solar wind exposure of $\sim 10^4$ – 10^5 years) resulted in the formation of amorphous "radiation-damaged" rims on the grain surfaces (summarized in Borg et al., 1980, 1983). At the same time, a number of investigators were debating the relative roles of sputter deposition and vapor deposition

(from impacts). These debates were undertaken in order to explain conflicting chemical and isotopic data obtained from the analysis of the grain surfaces, and fine size fractions of lunar soils. Theoretical considerations of the meteoroid flux interacting with the lunar surface lead to the inescapable conclusion that large amounts of vapor are produced by impact processes and are retained in the lunar regolith (Gault et al., 1972; Housley et al., 1973; Zook, 1975; Hapke and Cassidy, 1978; Cintala, 1992). The difficult task in understanding the nature of rims on lunar soil grains is being able to sort out the relative contributions of these various processes by some chemical or microstructural test.

We believe that the amorphous rims are produced mainly by the interaction of the soil grains with the solar wind. The microstructure and chemical systematics (particularly the oxygen superstoichiometry) are all consistent with recent experimental data on the irradiation of silicate surfaces (Bradley et al., 1996). Amorphous rims are predominantly an erosional feature of lunar soil grains, in that they record the preferential loss of ions by solar-wind sputtering. For plagioclase and pyroxenes, the results of solar wind irradiation are rim compositions that are different from the host grain, not in which elements are present, but in the relative proportions of those elements. For cristobalite, irradiation produces an amorphous rim which is compositionally identical to the host. These results indicate that on average in the lunar soil, irradiation results in the preferential loss of cations relative to Si and O which appear to sputter at nearly equivalent rates (this is also known from experimental sputtering experiments; see Hochella et al., 1988). If true, these results also would predict that deposition of sputtered elements would result in oxygen depletions in the deposit. For plagioclase, the relative sputtering rates are in the order (from the easiest to the most difficult) $Ca > Al > Si = O$, while in orthopyroxene the relative rates are $Mg > Ca = Al > Fe > Si = O$. Numerous studies have shown that preferential sputtering can occur to a certain depth and then the surface recedes by sputter erosion (e.g., Hochella et al., 1988).

It should be noted that in the data presented by Keller and McKay (1993), oxygen was not determined directly. Without knowledge of the true oxygen abundance in rims, real Ca- and Al-depletions, as observed in the example above, would appear as an apparent enrichment in Si and were reported as such. Citing older literature, Keller and McKay (1993) suggested that rims produced by irradiation would have the same composition as the host grain. It is now clear from both the results presented here as well as in

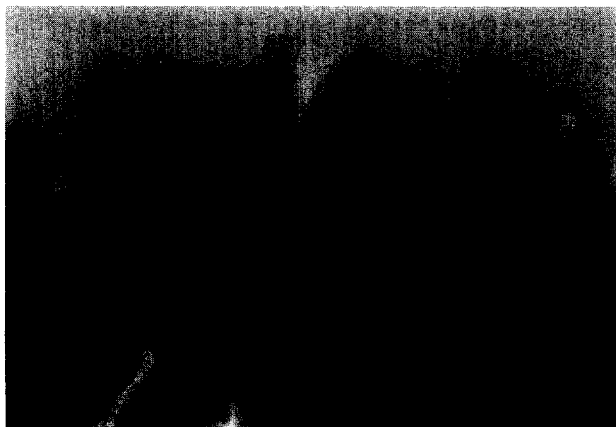


Fig. 8. A bright-field TEM image of a vesicular rim on pyroxene from soil 61221. The circular voids in the outer 100 nm of the grain are vesicles.

Table 4. Quantitative TEM-EDX analyses of typical vesicular rims and their substrates in lunar soils 61221 and 10084.

Analysis	(at%)	O	Mg	Al	Si	S	Ca	Ti	Fe
179	outer rim	66.9	4.20	1.38	21.4	0.02	3.54	0.28	2.3
178	inner rim	62.7	5.99	0.73	21.9	0.00	5.34	0.20	3.2
177	core (cpx)	59.1	8.20	0.84	20.9	0.04	7.12	0.16	3.7
137	rim	65.3	8.42	0.90	19.3	0.05	1.35	0.05	4.6
136	core (opx)	56.3	12.0	1.13	22.1	0.05	1.13	0.05	7.3
108	rim	62.2	2.83	11.4	16.0	0.10	6.70	0.00	0.8
109	core (glass)	60.7	5.05	10.8	16.5	0.03	5.60	0.07	1.2
111	rim	62.2	8.88	6.17	16.7	0.09	3.50	0.11	2.3
113	core (glass)	62.3	9.86	4.72	17.6	0.03	3.12	0.07	2.3
118	rim	59.4	6.98	4.73	15.9	0.15	4.84	4.15	3.9
117	core (opx)	58.0	9.56	1.54	20.3	0.00	6.70	0.60	3.3

the IDP literature, that irradiation of most silicates is not an isochemical process (the one clear exception is cristobalite, Table 1). However, the rim composition produced by irradiation of a substrate retains a memory of the substrate (i.e., an irradiated rim on an Mg-Fe pyroxene contains Mg, Fe, Si, and O, although the element ratios differ from the host pyroxene). The response of oxides (i.e., ilmenite) to solar wind irradiation is markedly different from what is observed in silicates. For ilmenite, solar-wind irradiation produced microcrystalline rims, not amorphous rims, and also resulted in the preferential removal of Fe and O from the outer few tens of nanometers of the ilmenite grains (Christoffersen et al., 1994; Bernatowicz et al., 1994a,b), along with a reduction of Fe²⁺ of Fe⁰ and Ti⁴⁺ to Ti³⁺ (Keller et al., 1995).

We interpret the inclusion-rich rims as a depositional feature of lunar soil grains. The presence of elements in the rims which are absent from the host demands that these elements were added to the grain surface. This is not a new hypothesis. For example, the unequivocal evidence for a major surface-correlated component of S in the lunar regolith requires the deposition of S via the condensation of impact-generated vapors or sputtered atoms (Kerridge et al., 1975; Rees and Thode, 1974; Keller and McKay, 1993). The elements and inclusions present in the inclusion-rich rims were clearly added to the surface of the grain by some process and, furthermore, the stratigraphy observed in the distribution of inclusions argues for an episodic process. The two main processes that have been proposed are sputter deposition, and the condensation of impact-generated vapors. The chemical composition of vapor-deposited materials is well constrained from numerous studies on the thermal evaporation of lunar materials (e.g., DeMaria et al., 1971; Hapke et al., 1975). Vapor deposits are deficient in oxygen and enriched in Si and Fe because of the deposition of species such as SiO and elemental Fe (two of the more volatile species). The composition of sputter-deposited materials is not as well constrained. Although early work suggested that there exists characteristic differences in the compositions of sputter-deposited material and vapor-deposited material (e.g., Hapke et al., 1975), these differences are not well understood, especially in regard to the behavior of oxygen. To our knowledge, no direct quantitative measurement of oxygen abundances in experimentally produced sputter deposits has been published. We can infer the chemical systematics of sputter deposits based upon the results of Bradley (1994a) and the

data presented here for amorphous rims. These results suggest that ferromagnesian silicates (olivine, pyroxene) preferentially lose Mg relative to the other ions during irradiation. Similarly, our data suggest that plagioclase suffers preferential sputtering of Ca and to a lesser extent Al, relative to both Si and O. Mass-balance constraints predict that these preferentially sputtered elements should accumulate in sputter deposits. If this hypothesis is correct, then sputter deposits should be enriched in the sputtered cations (especially Mg, Ca, and Al), and depleted in both oxygen and silicon. However, while oxygen depletions are observed, the inclusion-rich rims are consistently Si-rich, suggesting that the main source of the deposited material is impact generated vapors. We do not exclude the presence of sputter-deposited materials in rims of all types; however, our present set of data does not support a major component of sputter deposits in those rims that have been clearly deposited on soil grains. These interpretations require further experimental work in order to completely understand the chemical signature of sputter deposits as opposed to the deposition of impact-generated vapors. The situation is particularly complicated due to the variety of surfaces that are present for sputtering, including fresh grain surfaces, previously sputtered surfaces, and vapor-deposited coatings, all of which may respond differently to sputter erosion.

The inclusion-rich rims show either a random distribution of inclusions throughout the thickness of the rim or a distinct layering of inclusions. For those rims with a random distribution of inclusions, it appears that much of the rim material was deposited gradually and continuously over time (e.g., slow accretion), although the possibility also exists that the material in these rims was deposited in a single event. However, the layering of inclusions in many of the rims preserves evidence for multiple episodes of deposition (possibly fast accretion). The layering of inclusions suggests that material can be added to the surfaces in thickness intervals as thin as ~10 nm with up to ten distinct episodes of deposition.

The presence of multiple rims on soil grains is perhaps the best evidence that several processes are involved in rim formation. They also provide information on the thickness of material that can be deposited onto grain surfaces. For example, the multiple rim shown in Fig. 7 has a 40–50 nm thick inner layer that was produced by solar wind irradiation. The vapor-deposited material in the outer rim is also 40–50 nm thick. From these cases, it is clear that the radiation-

damaged (erosional) layer can be of comparable thickness to the vapor-deposited outer layer.

The presence of multiple rims on individual soil grains and the layering of Fe grains within inclusion-rich rims are strong arguments against the hypothesis that ion mixing is a major factor affecting the composition of rims. Ion mixing is the process where a pre-existing surface layer becomes homogenized with the substrate due to ion bombardment (Kelly and Sanders, 1976). In this way for example, the compositional difference between a surface layer that has undergone preferential sputtering can be mixed with unirradiated material at depth. It is unclear how the sharp compositional and microstructural boundaries in the multiple rims could be preserved if mixing over the ion range occurred with any degree of efficiency.

Vesicular rims on lunar soil grains also provide insight into regolith processes. The lack of a strong compositional difference between the vesicular rims and their hosts suggests that vapor deposition processes were at most minimally involved in their formation. Our current hypothesis is that these vesicular rims are related to the implantation of solar wind gases, either forming during the implantation, or by subsequent heating of the soil grains (heating from a nearby impact?). It is well known in the materials science literature that prolonged irradiation with a high fluence of ions can result in blistering and void formation in the surfaces of many materials (e.g., Hishmeh et al., 1994; Clinard and Farnum, 1993); however, it is difficult to derive scenarios where this fluence would be possible in the lunar regolith. The lack of major chemical differences between the vesicular rims and their hosts (particularly the lack of a large oxygen superstoichiometry) along with the apparent immaturity of the soil where they are common (61221) argues against long exposure with the nucleation and growth of noble gas bubbles. We believe that a more likely formation mechanism is the evolution of solar wind-implanted gases by a pulse-heating event that was of sufficient duration to nucleate vesicles, but short enough to avoid melting and vitrification of the entire host grain. Thus, we also need to consider whether a thermal event could modify the chemistry and microstructure of rims.

4.1. The Relative Roles of Erosional and Depositional Processes in Lunar Soils

Table A1 collects all of our TEM-EDX data for rims on lunar soil grains where we have obtained quantitative oxygen analyses for both the rim and host grain. The number of vesicular rims are statistically over-represented in the dataset, largely because they are so conspicuous in the thin sections. However, for the remaining rim analyses, we believe that they represent a reasonable sampling of rims on silicates in mature lunar soils. Using a combination of the oxygen stoichiometry, major element composition, and petrography (inclusions or no inclusions) we have classified the rims using the four rim types described above. For the twenty-five analyses of nonvesicular rims in Table A1, seven are classified as amorphous, seven are inclusion rich, seven are multiple, and four are classified as intermediate.

We have added the "intermediate" category because these rims do not fit neatly into any of the endmember types.

These rims show characteristics that are intermediate between typical amorphous and inclusion-rich rims. For example, the intermediate rims show little deviation (positive or negative) from stoichiometry with respect to oxygen. They usually contain deposited elements, but not in great abundance, and they typically contain minor submicroscopic Fe metal grains. While we favor this hypothesis, there are other alternatives. These rims could be related to the amorphous rims in that the intermediate rims may form largely from radiation damage that was sufficiently energetic to amorphize the rim, but not produce any preferential sputtering, combined with a slight addition of deposited elements. The possibility also exists that the intermediate rims are largely deposits of material that was completely vaporized (as opposed to fractionated vapors produced by partial vaporization). Until the appropriate experiments are conducted, it is not possible to determine which process or combination of processes formed these intermediate rims.

Provided that the statistics presented above for the dataset in Table A1 are representative of the rim types in mature lunar soils in general, then, the relative importance of vapor-deposition is comparable to radiation-damage in the formation of rims on lunar silicate grains. This conclusion is at odds with the results obtained on ilmenites from lunar soils. All analyzed ilmenites show pronounced element depletions (especially for Fe and O) in their surface layers (Christoffersen et al., 1994; Bernatowicz et al., 1994a,b), yet fewer than half of the silicate rims show such marked depletions. The vast majority of analyzed ilmenites contain only a minor deposited component (Bernatowicz et al., 1994a,b; Christoffersen et al., 1996) in contrast to the data for lunar silicates presented here. The differences between ilmenite and silicates are real, but it is not clear why these differences should exist. Ilmenites and silicates should receive the same radiation dose and be exposed to similar levels of impact-generated vapors (provided that their surface areas and residence times are comparable), and so the differences are not in how material is deposited on the grains, but rather depend on the retention of the deposits. Ilmenite may not retain vapor deposits with same efficiency as silicates because of the complex chemical reactions that occur in ilmenite surfaces due to the implantation of solar wind hydrogen (Christoffersen et al., 1996).

4.2. Implications For Space Weathering Processes

Reflectance spectra obtained from lunar soils show a reddened continuum, lower albedo, and weaker absorption features as compared to finely comminuted rocks from the same Apollo sites (Adams and McCord, 1970, 1971). Recent work has demonstrated that it is the finest size fraction (<25 μm) that dominates the optical properties of lunar soils (Pieters et al., 1993). Although it was generally assumed that the main darkening agent in lunar soils was agglutinitic glass (in particular, the submicroscopic Fe metal in agglutinitic glass), Pieters et al. (1993) demonstrated that agglutinitic glass alone could not account for the lowered albedo and reddened slope in reflectance spectra, and suggested that a surface correlated material was the main factor in accounting for the reddened continuum slope in lunar soils. We believe that the inclusion-rich rims on lunar soil grains

are the most likely candidate material that is responsible for the main optical properties of the lunar soil. This hypothesis is supported both by the work of Pieters et al. (1993) and the results of Allen et al. (1996) who demonstrated that the Fe metal grains must be very small (<10 nm) in order to cause appreciable reddening of reflectance spectra. If the Fe grains are too large, they cause darkening without adding a red slope to spectra (Allen et al., 1996). Further support comes from the measurement of the characteristic ferromagnetic resonance (FMR) intensity in immature soils (Morris, 1977). The FMR data suggest that the fine-grained Fe metal is surface-correlated in immature soils, and evolves to a volume-correlated component in more mature soils through the formation of agglutinate particles. Clearly, experiments are required that duplicate lunar regolith processes that modify grain surfaces, followed by measurement of reflectance spectra and detailed characterization of the grain surfaces. In this way, it would be possible to verify whether 50–100 nm thick coatings on grain surfaces have the potential to strongly modify the optical properties of the lunar soil.

5. CONCLUSIONS

TEM analysis of the rims surrounding lunar soil grains allows the rims to be grouped into four broad classes based on their microstructure and chemistry. Amorphous rims lack crystallinity, are essentially devoid of crystalline inclusions, display a unique chemical signature of irradiation processes (i.e., oxygen superstoichiometry, except for cristobalite), and formed as a result of solar wind irradiation damage. Inclusion-rich rims are the other major rim type observed in lunar soils and are characterized by an abundance of nanometer-sized inclusions of Fe-metal, ilmenite, and other opaque phases as random inclusions or in discrete layers embedded in an amorphous, silicate matrix. The chemistry of inclusion-rich rims is most consistent with deposition of impact-generated vapors (oxygen substoichiometry), although a component of sputter deposition cannot be excluded. There exists a continuum between “pure” amorphous rims and “pure” inclusion-rich rims. Multiple-rims typically consist of a discrete radiation damaged layer that is overlain by a layer of vapor-deposited material. Vesicular rims are formed by the evolution of solar wind–implanted gases during a pulse-heating event.

The surfaces of lunar soil grains can be eroded by the action of the solar wind, material can be deposited through vapor- or sputter deposition, or both processes may operate simultaneously. The fact that both erosional and depositional processes are operating in the lunar regolith indicates that one cannot use rim thicknesses for detailed analysis of past solar activity unless there is verification that the rim thickness is only due to radiation damage. This study indicates that this needs to be determined on a grain by grain basis.

The presence of abundant, submicroscopic Fe metal grains in inclusion-rich rims may have a profound impact on the optical and magnetic properties of the lunar soil. The inclusion-rich rims are the best candidate yet identified in lunar soils as the cause of the reddened continuum slope of lunar soils.

Acknowledgments—This manuscript benefited from careful and detailed reviews by T. Bernatowicz, G. J. Flynn, and J. F. Kerridge, and the editorial comments of Ghislane Crozaz. This work was

supported by NASA RTOP 152-17-40-21 (DSM) and NASA Contract NAS 9-18992 (LPK).

Editorial handling: G. Crozaz

REFERENCES

- Adams J. B. and McCord T. B. (1970) Remote sensing of lunar surface mineralogy: Implications from visible and near infrared reflectivity of Apollo 11 samples. *Geochim. Cosmochim. Acta* (Suppl. 1), 1937–1945.
- Adams J. B. and McCord T. B. (1971) Alteration of lunar optical properties: Age and compositional effects. *Science* **171**, 567–571.
- Allen C. C., Morris R. V., and McKay D. S. (1996) An experimental analog to maturing lunar soil. *Lunar Planet. Sci. Conf. XXVII*, 13–14 (abstr.).
- Bernatowicz T. J., Nichols R. H., and Hohenberg C. M. (1994a) Origin of amorphous rims on lunar soil grains. *Lunar Planet. Sci. Conf. XXV*, 105–106 (abstr.).
- Bernatowicz T. J., Nichols R. H., Hohenberg C. M., and Maurette M. (1994b) Vapor deposits in the lunar regolith: Technical comment. *Science* **264**, 1779–1780.
- Bibring J.-P., Durand J. P., Durrieu L., Jouret C., Maurette M., and Meunier R. (1972) Ultrathin amorphous coatings on lunar dust grains. *Science* **175**, 753–755.
- Bibring J.-P., Langevin Y., and Rocard F. (1982) Synthesis of molecules by irradiation in silicates. *Proc. 13th Lunar Planet. Sci. Conf.*, A446–A450.
- Borg J., Chaumont J., Jouret C., Langevin Y., and Maurette M. (1980) Solar wind radiation damage in lunar dust grains and the characteristics of the ancient solar wind. In *Proceedings of the Conference on the Ancient Sun*, 431–461.
- Borg J., Bibring J.-P., Cowsik G., Langevin Y., and Maurette M. (1994b) A model for the accumulation of solar wind radiation damage effects in lunar dust grains, based on recent results concerning implantation and erosion effects. *Proc. 13th Lunar Planet. Sci. Conf.*, A725–A730.
- Bradley J. P. (1994a) Chemically anomalous, preaccretionally irradiated grains in interplanetary dust from comets. *Science* **265**, 925–929.
- Bradley J. P. (1994b) Nanometer-scale mineralogy and petrography of fine-grained aggregates in anhydrous interplanetary dust particles. *Geochim. Cosmochim. Acta* **58**, 2123–2134.
- Bradley J. P., Dukes C., Baragiola R., McFadden L., Johnson R. E., and Brownlee D. E. (1996) Radiation processing and the origins of interplanetary dust. *Lunar Planet. Sci. Conf. XXVII*, 149–150 (abstr.).
- Christoffersen R., McKay D. S., and Keller L. P. (1994) Grain rims on ilmenite in the lunar regolith: comparison to vapor deposits on regolith silicates. *Lunar Planet. Sci. Conf. XXV*, 259–260 (abstr.).
- Christoffersen R., Keller L. P., and McKay D. S. (1996) Microstructure, chemistry, and origin of grain rims on ilmenite from the lunar soil finest fraction. *Meteoritics and Planetary Science* **31**, 835–848.
- Cintala M. J. (1992) Impact-induced thermal effects in the Lunar and Mercurian regoliths. *J. Geophys. Res.* **97**, 947–973.
- Clayton R. N., Mayeda T., and Hurd J. M. (1974) Loss of oxygen, silicon, sulfur, and potassium from the lunar regolith. *Proc. 5th Lunar Planet. Sci. Conf.*, 1801–1809.
- Clinard F. W. and Farnum E. H. (1993) Irradiation effects in ceramics: transition from low to high dose behavior. *J. Nucl. Materials* **206**, 353–359.
- DeMaria G., Balducci G., Guido M., and Piacente V. (1971) Mass spectrometric investigation of the vaporization process of Apollo 12 lunar samples. *Proc. 2nd Lunar Planet. Sci. Conf.* 1367–1380.
- Dikov Y. P. et al. (1978) Some features of the main element conditions in surface layers of regolith particles of the Luna automatic stations samples: X-ray photoelectronic spectroscopy studies. *Proc. 9th Lunar Planet. Sci. Conf.*, 2111–2124.
- Dran J. C., Durrieu L., Jouret C., and Maurette M. (1970) Habit and texture studies of lunar and meteoritic material with the 1 MeV electron microscope. *Earth Planet. Sci. Lett.* **9**, 391–400.
- Epstein S. and Taylor H. P. (1972) O^{18}/O^{16} , Si^{30}/Si^{28} , C^{13}/C^{12} ,

- and D/H studies of Apollo 14 and 15 samples. *Proc. 3rd Lunar Planet. Sci. Conf.*, 1429–1454.
- Esat T. M. and Taylor S. R. (1992) Magnesium isotope fractionation in lunar soils. *Geochim. Cosmochim. Acta* **56**, 1025–1031.
- Fallick A. E., Pillinger C. T., Stephenson A., and Housley R. M. (1983) Concerning the size distribution of ultrafine iron in lunar soil. *Lunar Planet. Sci. Conf. XIV*, 245–246 (abstr.).
- Gault D. E., Horz F., and Hartung J. B. (1972) Effects of microcratering on the lunar surface. *Proc. 3rd Lunar Planet. Sci. Conf.*, 2713–2734.
- Gold T., Bilson E., and Baron R. L. (1975) Auger analysis of lunar soils: Study of processes which change the surface chemistry and albedo. *Proc. 6th Lunar Planet. Sci. Conf.*, 3285–3303.
- Hapke B. and Cassidy W. (1978) Is the Moon really as smooth as a billiard ball? Remarks concerning recent models of sputter-fractionation on the lunar surface. *Geophys. Res. Lett.* **5**, 297–300.
- Hapke B., Cassidy W., and Wells E. (1975) Effects of vapor-phase deposition processes on the optical, chemical, and magnetic properties of the lunar regolith. *The Moon* **13**, 339–353.
- Hishmeh G. A., Cartz L., Desage F., Templier C., Desoyer J. C., and Bircher R. C. (1994) Rare gas bubbles in muscovite mica implanted with xenon and krypton. *J. Materials Res.* **9**, 127–136.
- Hochella M. F., Jr., Lindsay J. R., Mossotti G., and Eggleston C. M. (1988) Sputter depth profiling in mineral-surface analysis. *Amer. Mineral.* **73**, 1449–1456.
- Housley R. M. and Grant R. W. (1976) ESCA studies of the surface chemistry of lunar fines. *Proc. 7th Lunar Planet. Sci. Conf.*, 881–889.
- Housley R. M. and Grant R. W. (1977) An XPS (ESCA) study of lunar surface alteration profiles. *Proc. 8th Lunar Planet. Sci. Conf.*, 3885–3899.
- Housley R. M., Grant R. W., and Paton N. E. (1973) Origin and characteristics of excess Fe metal in lunar glass welded aggregates. *Proc. 4th Lunar Planet. Sci. Conf.*, 2737–2749.
- Keller L. P. and McKay D. S. (1993) Discovery of vapor deposits in the lunar regolith. *Science* **261**, 1305–1307.
- Keller L. P. and McKay D. S. (1994a) The contribution of vapor deposition to amorphous rims on lunar soil grains. *Meteoritics* **29**, 480 (abstr.).
- Keller L. P. and McKay D. S. (1994b) Vapor deposits in the lunar regolith: Technical comment. *Science* **264**, 1780.
- Keller L. P. and McKay D. S. (1994c) The nature of agglutinitic glass in the fine size fraction of lunar soil 10084. *Lunar Planet. Sci. Conf. XXV*, 685–686 (abstr.).
- Keller L. P., Christoffersen R., and McKay D. S. (1995) The oxidation state of altered rims ilmenite from lunar soils. *Lunar Planet. Sci. Conf. XXV*, 729–730.
- Kelly R. and Sanders J. B. (1976) On the role of recoil implantation in altering the stoichiometry of a bombarded solid. *Nuclear Instruments and Methods in Physics Research, Section B: Beam interactions with Materials and Atoms* **132**, 335–343.
- Kerridge J. F. and Kaplan I. R. (1978) Sputtering: Its relationship to isotopic fractionation on the lunar surface. *Proc. 9th Lunar Planet. Sci. Conf.*, 1687–1710.
- Kerridge J. F., Kaplan I. R., and Petrowski C. (1975) Evidence for meteoritic sulfur in the lunar regolith. *Proc. 6th Lunar Planet. Sci. Conf.*, 2151–2162.
- McKay D. S., Heiken G., Basu A., Blanford G., Simon S., Reedy R., French B. M., and Papike J. (1991) The lunar regolith. In *Lunar Sourcebook: A User's Guide to the Moon* (ed. G. Heiken et al.), pp. 285–356. Cambridge Univ. Press.
- Morris R. V. (1977) Origin and evolution of the grain-size dependence of the concentration of fine-grained metal in lunar soils: The maturation of soils to a steady-state stage. *Proc. 8th Lunar Planet. Sci. Conf.*, 3719–3747.
- Pieters C. M., Fischer E. M., Rode O., and Basu A. (1993) Optical effects of space weathering: The role of the finest fraction. *J. Geophys. Res.* **98**, 20817–20824.
- Rees C. E. and Thode H. G. (1974) Sulfur concentrations and isotope ratios in Apollo 16 and 17 samples. *Proc. 5th Lunar Planet. Sci. Conf.*, 1963–1974.
- Russell W. A., Papanastassiou D. A., and Tombrello T. A. (1977) Ca isotope fractionation on the moon. *Proc. 8th Lunar Planet. Sci. Conf.*, 3791–3805.
- Walker R. M. (1980) Nature of the fossil evidence: Moon and meteorites. In *The Ancient Sun: Fossil Record in the Earth, Moon, and Meteorites* (ed. R. O. Pepin et al.), pp. 11–28. Pergamon.
- Zeller E. J., Ronca L. B., and Levy P. W. (1966) Proton induced hydroxyl formation on the lunar surface. *J. Geophys. Res.* **71**, 4855–4860.
- Zinner E., Dust S., Chaumont J., and Dran J. C. (1978) Surface concentrations of Mg, Ti, Fe and surface features in individual plagioclase crystals from lunar soil samples. *Proc. 9th Lunar Planet. Sci. Conf.*, 1667–1686.
- Zook H. A. (1975) The state of meteoritic material on the Moon. *Proc. 6th Lunar Planet. Sci. Conf.*, 1653–1672.

Table A1. Quantitative TEM-EDX analysis of amorphous rims and their substrates in Apollo 11 and 17 soils.

Analysis (at%)	Type*	O	Na	Mg	Al	Si	S	Ca	Ti	Fe
242 rim	I-R	52.7	n.d.	5.36	12.4	18.5	0.04	7.03	0.50	3.54
243 core (An)		61.0	n.d.	0.51	15.6	16.2	0.00	6.74	0.00	0.00
240 rim	inter	65.0	n.d.	1.16	7.65	23.2	0.02	1.18	0.58	1.24
241 core (opx)		60.3	n.d.	12.8	3.44	17.5	0.01	2.00	0.20	3.80
26 rim	inter	62.8	n.d.	2.14	4.99	25.1	0.31	1.73	0.81	2.06
25 core (cpx)		59.8	n.d.	6.62	1.47	20.2	0.03	4.40	0.29	7.21
21 rim	I-R	60.9	n.d.	3.59	4.13	25.9	0.27	1.68	0.72	2.82
20 core (opx)		60.2	n.d.	13.3	0.53	20.5	0.00	1.50	0.16	3.91
46 outer rim	I-R	60.5	n.d.	3.61	7.20	18.7	0.41	3.56	1.18	4.72
45 inner rim	I-R	59.9	n.d.	2.94	11.2	18.1	0.22	5.00	0.61	2.10
44 core (An)		61.6	n.d.	0.16	14.8	15.9	0.00	7.58	0.00	0.01
34 outer rim	AM	67.7	n.d.	3.43	2.49	21.9	0.38	0.81	0.53	2.80
35 inner rim	AM	59.7	n.d.	6.88	2.93	26.5	0.14	1.15	0.12	2.55
36 core (opx)		60.2	n.d.	14.9	0.31	19.8	0.01	0.84	0.07	3.94
208 rim	inter	64.7	n.d.	4.88	3.16	20.3	0.07	4.05	0.40	2.49
209 core (opx)		60.5	n.d.	9.79	0.72	19.9	0.07	2.78	0.25	5.99
211 rim	AM	68.6	n.d.	0.58	7.16	21.8	0.00	1.52	0.00	0.29
210 core (An)		60.8	n.d.	0.40	15.7	15.8	0.00	7.30	0.00	0.01
214 rim	inter	58.4	n.d.	0.92	10.5	22.8	0.14	3.10	0.40	3.75
213 core (An)		62.3	n.d.	0.45	14.4	16.1	0.00	6.79	0.00	0.00
217 outer rim	I-R	66.3	n.d.	0.80	5.89	23.3	0.04	1.36	0.15	2.14
216 inner rim	AM	68.3	n.d.	0.49	8.48	19.9	0.03	2.04	0.07	0.69
215 core (An)		62.1	n.d.	0.45	15.0	15.6	0.00	6.92	0.00	0.02
218 outer rim	I-R	67.0	n.d.	0.00	4.78	24.9	0.00	0.76	0.97	1.58
219 inner rim	I-R	67.7	n.d.	0.38	3.43	28.2	0.01	0.20	0.03	0.01
220 core (crst)		65.0	n.d.	0.01	0.18	34.9	0.00	0.00	0.00	0.00
120 rim	I-R	60.6	0.17	2.79	9.53	17.8	0.30	3.66	0.57	4.60
121 core (An)		59.2	1.31	0.38	14.8	17.9	0.01	6.42	0.00	0.00
111 outer rim	I-R	60.8	0.40	3.22	5.98	12.0	0.09	3.04	7.18	7.19
113 inner rim	AM	59.1	0.60	1.09	14.8	19.4	0.00	3.73	0.39	0.89
112 core (An)		59.6	0.67	0.74	15.5	16.7	0.00	6.75	0.00	0.08
70 outer rim Fe	I-R	63.9	n.d.	3.47	5.73	16.1	0.16	3.67	1.43	5.57
69 outer rim	AM	63.8	n.d.	3.46	4.82	16.2	0.05	4.24	0.90	6.45
68 inner rim Fe	I-R	60.9	n.d.	3.02	3.40	17.0	0.00	5.30	0.95	9.47
67 inner rim	AM	61.5	n.d.	3.07	3.67	17.1	0.09	4.98	0.76	8.91
65 core (opx)		61.7	n.d.	12.2	0.38	18.8	0.08	0.92	0.13	5.93
152 outer rim	I-R	57.5	n.d.	6.65	7.67	18.5	0.19	3.89	1.21	4.44
151 inner rim	AM	63.4	n.d.	0.28	11.0	22.2	0.00	3.11	0.00	0.07
150 core (An)		62.6	n.d.	0.1	14.9	15.1	0.00	7.22	0.00	0.00
155 outer rim	I-R	58.3	n.d.	5.96	5.31	14.7	0.20	4.54	4.36	6.67
154 inner rim	AM	62.2	n.d.	0.76	11.9	20.6	0.04	3.69	0.34	0.50
153 core (An)		60.7	n.d.	0.18	15.8	16.0	0.00	7.28	0.00	0.04
157 rim	AM	63.5	n.d.	0.63	10.9	20.1	0.07	2.89	0.06	1.90
156 core (An)		61.2	n.d.	0.52	15.7	15.5	0.06	7.00	0.00	0.03
163 outer rim	I-R	60.1	n.d.	3.93	7.70	20.4	0.30	4.67	0.18	2.66
162 mid rim	I-R	54.1	n.d.	6.17	9.42	20.5	0.16	6.02	0.29	3.33
160 inner rim	I-R	52.6	n.d.	3.78	8.10	26.5	0.26	4.81	0.18	3.74
159 core (An)		59.7	n.d.	0.55	15.6	16.6	0.06	7.42	0.02	0.06
165 rim	I-R	57.0	n.d.	5.75	7.58	18.2	0.21	4.63	1.38	5.29
164 core (Aug)		59.0	n.d.	8.11	0.84	19.0	0.00	5.26	0.22	7.57
171 outer rim	I-R	57.8	n.d.	6.75	9.24	16.3	0.31	4.55	0.73	4.35
172 inner rim	AM	63.6	n.d.	0.39	0.64	34.8	0.04	0.23	0.05	0.24
170 core (crst)		65.3	n.d.	0.04	0.40	34.2	0.00	0.00	0.00	0.00
6159 rim	AM	58.5	n.d.	0.85	1.41	37.3	0.00	0.69	0.36	0.89
6158 core (crst)		63.5	n.d.	0.39	0.68	35.2	0.00	0.09	0.02	0.11
6165 rim	AM	62.0	n.d.	1.32	6.69	21.7	0.44	2.49	1.81	3.64
6166 core (An)		61.0	n.d.	0.03	15.0	16.8	0.00	7.24	0.00	0.00
6167 rim	AM	62.0	n.d.	8.65	1.36	20.8	0.38	1.19	0.47	5.16
6168 core (opx)		61.7	n.d.	10.2	1.09	19.3	0.00	2.22	0.34	5.10
6185 rim	AM	64.3	n.d.	0.2	0.32	35.2	0.00	0.01	0.00	0.01
6184 core (crst)		63.8	n.d.	0.18	0.37	35.6	0.00	0.06	0.00	0.00
57 outer rim	I-R	56.2	n.d.	1.50	1.70	14.3	0.33	0.90	17.3	7.80
58 inner rim	AM	61.8	n.d.	1.60	0.30	2.0	0.21	0.10	30.3	3.50
60 core (ilm)		62.9	n.d.	0.80	0.00	0.4	0.00	0.00	18.9	17.0
179 outer rim	V	66.9	n.d.	4.20	1.38	21.4	0.02	3.54	0.28	2.3
178 inner rim	V	62.7	n.d.	5.99	0.73	21.9	0.00	5.34	0.20	3.2
177 core (cpx)	V	59.1	n.d.	8.20	0.84	20.9	0.04	7.12	0.16	3.7
137 rim	V	65.3	n.d.	8.42	0.90	19.3	0.05	1.35	0.05	4.6
136 core (opx)		56.3	n.d.	12.0	1.13	22.1	0.05	1.13	0.05	7.3
108 rim	V	62.2	n.d.	2.83	11.4	16.0	0.10	6.70	0.00	0.8
109 core (glass)		60.7	n.d.	5.05	10.8	16.5	0.03	5.60	0.07	1.2
111 rim	V	62.2	n.d.	8.88	6.17	16.7	0.09	3.50	0.11	2.3
113 core (glass)		62.3	n.d.	9.86	4.72	17.6	0.03	3.12	0.07	2.3
118 rim	V	59.4	n.d.	6.98	4.73	15.9	0.15	4.84	4.15	3.9
117 core (opx)		58.0	n.d.	9.56	1.54	20.3	0.00	6.70	0.60	3.3

* Rim types: I-R = inclusion-rich, AM = amorphous, V = vesicular, and inter = intermediate.